Sensors and Materials, Vol. 35, No. 2 (2023) 545–551
MYU Tokyo

S & M 3193

Shape Control of Small Li Glass Composite Scintillator for Optical-fiber-based Detectors

Yuya Oshima,[1*] Kenichi Watanabe,[1] Hiroshi Shiga,[2] and Genichiro Wakabayashi[2]

[1]Department of Applied Quantum Physics and Nuclear Engineering, Kyushu University,
744 Motooka, Nishi-ku, Fukuoka 819-0395, Japan
[2]Atomic Energy Research Institute, Kindai University, 3-4-1 Kowakae, Higashi-Osaka, Osaka 577-8502, Japan

(Received September 30, 2022; accepted January 18, 2023)

Keywords: neutron detector, Li glass scintillator, optical fiber, transparent composite scintillator, boron neutron capture therapy

Boron neutron capture therapy (BNCT) is one of the radiation therapies using neutrons. In BNCT, neutron monitoring is essential to ensure safety and evaluate the effect of treatments. As a neutron monitor for BNCT, we are developing an optical-fiber-based neutron detector using a small Li glass scintillator. This type of detector shows a clear neutron peak in the pulse height spectrum and has a high counting-rate capability owing to its short decay time. However, the sensitivity of the detector is uncontrollable owing to its random scintillator shape. In this study, we propose a Li glass transparent composite scintillator, in which Li glass grains and UV-curable resin are mixed, to realize a small and shape-controlled scintillator. We first fabricated the Li glass transparent composite scintillator and then experimentally confirmed that its response showed a clear neutron peak. We also fabricated an optical-fiber-based neutron detector using the Li glass transparent composite scintillator. The scintillator was formed into a hemispherical shape at the tip of an optical fiber. We confirmed the response of the optical-fiber-based detector, which showed a clear neutron peak. The experimentally evaluated sensitivity of the fabricated optical-fiber-based detector roughly agreed with the sensitivity estimated from its shape and size. Therefore, we conclude that the sensitivity of the optical-fiber-based neutron detector can be roughly controlled by using the Li glass transparent composite scintillator.

1. Introduction

Boron neutron capture therapy (BNCT) is a radiation therapy using neutrons and is a promising treatment for malignant cancer.(1–4) In BNCT, a boron agent is first administered to a patient and it accumulates in tumor cells. The patient is then externally irradiated with neutrons to induce $^{10}B(n, \alpha)^{7}Li$ reactions in these cells, which are selectively attacked by energetic charged particles such as alpha particles and ^{7}Li ions because of their short ranges of 9 and 4.5 mm, respectively. A neutron monitoring technique plays an important role in confirming and characterizing the irradiation field in BNCT. Since neutrons play an important role in BNCT,

*Corresponding author: e-mail: oshima.yuya.140@s.kyushu-u.ac.jp
https://doi.org/10.18494/SAM4148

ISSN 0914-4935 © MYU K.K.
https://myukk.org/

neutron monitoring is required to control exposure to medical radiation. Neutron monitors for BNCT are required to accept a high flux of neutrons of up to 10^9 n/cm^2/s and to cause little interference of the irradiation field. To meet these requirements, we have developed optical-fiber-based neutron detectors that combine a small neutron scintillator and an optical fiber.

An original version of the developed optical-fiber-based neutron detector used a bright Eu:$LiCaAlF_6$ scintillator.[5–12] Although the Eu:$LiCaAlF_6$ scintillator has a reasonably high light yield, its relatively long decay time limits its counting-rate capability. Consequently, the scintillator size or the number of ^{6}Li atoms in a scintillator should be sufficiently small to prevent counting loss even in an intense BNCT neutron field. Since the sensitivity of this type of detector is rather low, it is difficult to calibrate the sensitivity at a standard neutron field, in which the neutron flux is accurately evaluated but generally not particularly high.

To overcome the problem of low sensitivity, we used a Li glass scintillator, which has a shorter decay time than a Eu:$LiCaAlF_6$ scintillator, in an optical-fiber-based neutron detector.[13–16] By using a fast Li glass scintillator, the dynamic range of the detector counting rate was extended up to 1 Mcps. This feature allows the scintillator size or the detection sensitivity to be increased. Another notable advantage of the developed detectors is that a clear peak corresponding to neutron events appears in the pulse height spectrum. Owing to this feature, it is easy to check the signal gain or normal operation of the detector and to determine its sensitivity.

For medical uses, it is particularly desirable for neutron monitors to be accurately calibrated at a standard neutron field. In this calibration procedure, it is desirable to monitor the detector responses, such as the sensitivity, the wall effect, and the self-shielding effect, using Monte Carlo simulations. However, since the small scintillators used in the previously developed detectors had random shapes, it was difficult to accurately model them in the Monte Carlo simulations.

In this study, we propose the use of a Li glass transparent composite scintillator, in which Li glass powder and UV-curable resin are mixed, in an optical-fiber-based neutron detector. It is easy to control the shape of this type of scintillator. We first evaluate the response of a Li glass transparent composite scintillator to thermal neutron irradiation. We then fabricate an optical-fiber-based neutron detector using the Li glass transparent composite scintillator and experimentally evaluate the neutron response of the fabricated detector.

2. Materials and Methods

2.1 Li glass transparent composite scintillator

A Li glass transparent composite scintillator was fabricated by mixing Li glass scintillator (GS20) powder and UV-curable resin (HayacoatUV). The GS20 scintillator, in which the isotopic abundance of ^{6}Li is enriched to 95%, has a short decay time of 75 ns. First, a Li glass scintillator was grained using an automatic mortar. Scintillator grains with sizes ranging from 45 to 63 μm were selected using sieves. Then, the Li glass powder and UV-curable resin were mixed with a weight ratio of 2:1. The mixed resin is easily shaped by molding or its surface tension. The mixed resin was placed in a flexible silicone mold and then solidified by irradiating UV light. Figure 1

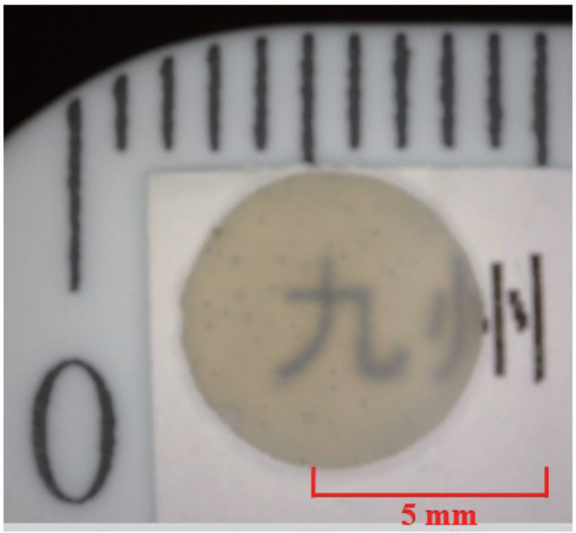

Fig. 1. (Color online) Photograph of the fabricated disk-shaped Li glass transparent composite scintillator.

shows a photograph of the fabricated Li glass transparent composite scintillator. The fabricated scintillator was disk-shaped with a diameter of 6 mm and a thickness of 1 mm. It was mounted on a photoelectric window of a photomultiplier tube (PMT, R7600U-200, Hamamatsu). The anode signal of the PMT was fed into a digital multichannel analyzer (digital MCA, HSDMCA4M4N17, ANSeeN). The digital MCA determined the signal pulse height of each event and transferred the list-mode data to a control PC. The pulse height spectrum was generated in the control PC.

To evaluate the neutron response, the fabricated detector was irradiated with neutrons emitted from a ^{252}Cf source surrounded by a polyethylene moderator. Figure 2 shows the experimental setup. To confirm the thermal neutron response, we also measured the pulse height spectrum when shielding neutrons using a Cd plate, which can selectively absorb thermal neutrons. We also obtained the pulse height spectrum obtained from a bulk Li glass scintillator as a comparison.

2.2 Optical-fiber-based neutron detector

We also fabricated an optical-fiber-based neutron detector using the Li glass transparent composite scintillator described above. A mixture of Li glass powder and UV-curable resin was placed at the tip of a quartz optical fiber (FP600URT, Thorlabs) with a transmission loss of 70 dB/km for the emission wavelength of the Li glass scintillator, a numerical aperture of 0.5, a core diameter of 600 μm, and a length of 10 m. The composite resin spontaneously formed a hemispherical shape due to surface tension. The composite was then solidified by irradiating UV light. Figure 3 shows a photograph of the Li glass transparent composite scintillator formed at the tip of an optical fiber. The scintillator region was then coated with TiO_2 powder as a diffusive reflector. The detector head was shielded from ambient light by a black heat-shrink

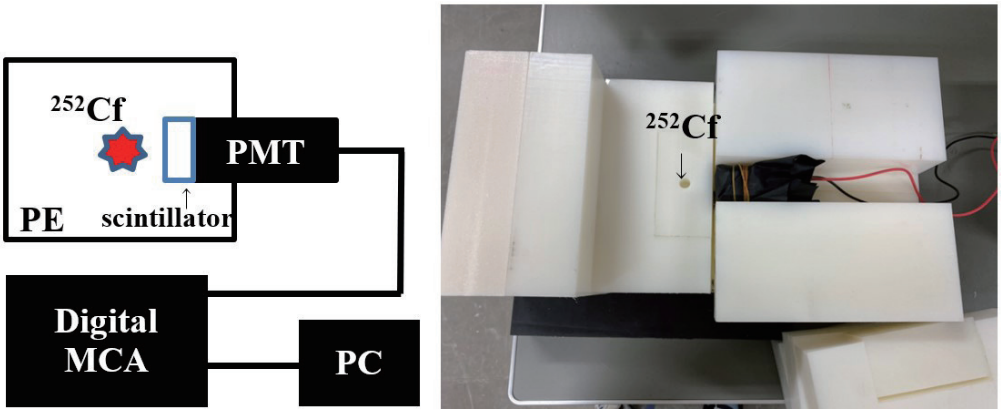

Fig. 2. (Color online) Experimental setup of the neutron response evaluation of the disk-shaped Li glass transparent composite scintillator.

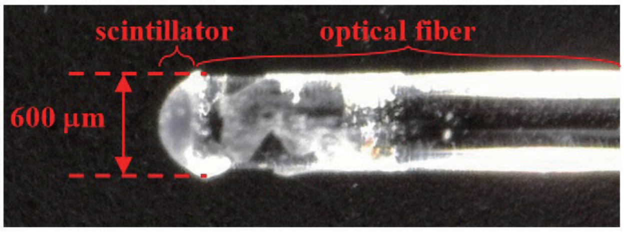

Fig. 3. (Color online) Photograph of the Li glass transparent composite scintillator formed at the tip of an optical fiber.

tube. The other end of the optical fiber was connected to a PMT (R9880U-210, Hamamatsu). The PMT signal was fed into the signal processing unit described above.

The neutron response evaluation experiments were conducted at the research nuclear reactor UTR-KINKI of the Atomic Energy Research Institute of Kindai University. The detector probe was inserted into the central stringer hole of the reactor, in which the neutron flux was 1.2×10^7 n/cm^2/s at a reactor power of 1 W.

3. Results and Discussion

3.1 Neutron response of disk-shaped Li glass transparent composite scintillator

Figure 4 shows the pulse height spectra obtained from the disk-shaped Li glass transparent composite and the bulk Li glass scintillator when irradiating neutrons. The detector counts are normalized by the peak counts. A clear peak is confirmed in the pulse height spectrum. Since the peak count markedly decreased upon the Cd neutron shielding, the peak component can be considered to correspond to neutron events. The signal pulse height of the neutron peak obtained by the transparent composite scintillator was half that obtained by the bulk Li glass scintillator. This is considered to be because the energy released by charged particles generated in ^{6}Li(n, t)α

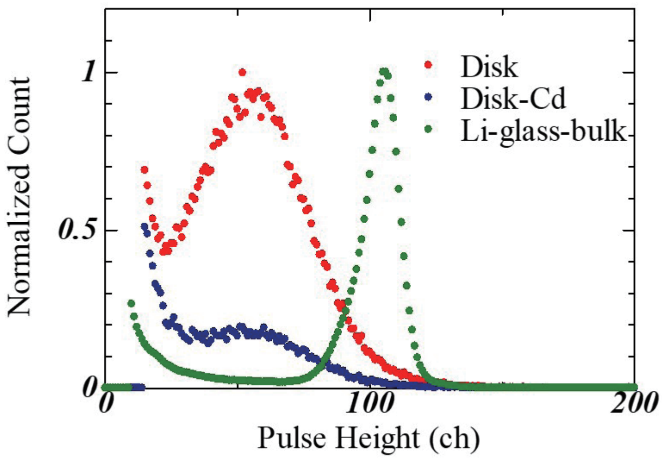

Fig. 4. (Color online) Pulse height spectra obtained from the disk-shaped Li glass transparent composite and the bulk Li glass scintillator when irradiating neutrons. The spectrum obtained from the bulk Li glass scintillator is also plotted for comparison.

reactions is partially deposited on the Li glass scintillator grains and because the transparency of the composite scintillator is lower than that of the bulk one. Although the peak pulse height and width are smaller and larger than those of the bulk Li glass, respectively, the Li glass transparent composite scintillator is confirmed to create a clear neutron peak, which makes it easy to set the discrimination level and determine the detector sensitivity.

3.2 Evaluation of neutron response to optical-fiber-based neutron detector

Figure 5 shows the pulse height spectra due to neutrons for the optical-fiber-based neutron detector. As with the disk-shaped transparent composite scintillator, clear peaks can be seen. Its application to optical fibers is considered to be feasible.

We can determine the neutron sensitivity of the fabricated optical-fiber-based detector from the peak area. The peak area count rate was 2300 cps at the reactor power of 1 W, which corresponds to a neutron flux of 1.2×10^7 n/cm^2/s. In this case, since the lower side of the neutron peak overlapped with the gamma-ray or noise component, the peak area was derived from twice the count integrated from the peak pulse height to the upper limit, that is, twice the upper half area of the peak. Consequently, the neutron sensitivity was evaluated to be 1.9×10^{-4} cps/(n/cm^2/s). On the other hand, the sensitivity can be estimated from the number of ^{6}Li atoms contained in the composite scintillator and the thermal neutron absorption cross section. The volume of the composite scintillator was estimated to be 3.7×10^{-5} cm^3 from Fig. 3. By considering the composition of the composite scintillator, the number of ^{6}Li atoms contained in the scintillator was determined to be 1.6×10^{17} atoms. Therefore, the thermal neutron sensitivity was estimated to be 1.5×10^{-4} cps/(n/cm^2/s). The estimated sensitivity roughly agreed with the experimentally evaluated value. From this comparison, we concluded that the sensitivity of the optical-fiber-based neutron detector using the Li glass transparent composite scintillator can be roughly controlled because the scintillator shape at the optical fiber tip can be controlled using the UV-curable composite.

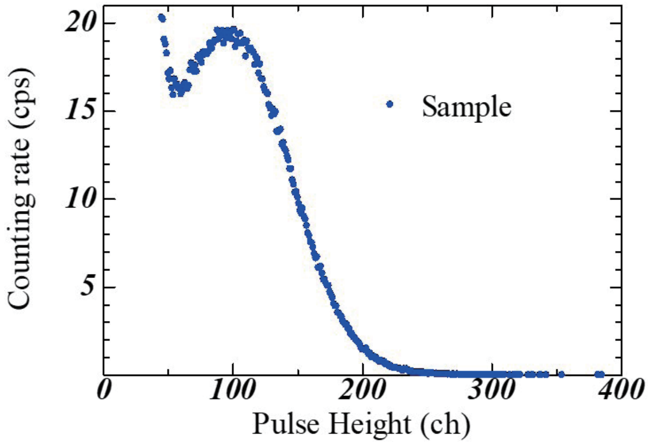

Fig. 5. (Color online) Pulse height spectra obtained from the optical-fiber-based neutron detector using the Li glass transparent composite scintillator when irradiating neutrons.

4. Conclusions

We proposed a Li glass transparent composite scintillator, which is a mixture of Li glass scintillator grains and UV-curable resin, as a small and shape-controllable scintillator for optical-fiber-based neutron detectors. First, we fabricated a disk-shaped Li glass transparent composite scintillator and experimentally evaluated its neutron response. The fabricated scintillator showed a clear neutron peak in the pulse height spectrum. This feature makes it easy to set the discrimination level and determine the detector sensitivity. We also fabricated an optical-fiber-based neutron detector using the Li glass transparent composite scintillator. This type of detector also showed a clear neutron peak. The detector sensitivity was experimentally determined to be 1.9×10^{-4} cps/(n/cm^2/s). Since the composite scintillator shape was controlled, it was easy to determine the number of ^{6}Li atoms contained in the scintillator. The sensitivity estimated from the scintillator shape and size roughly agreed with the experimentally determined sensitivity. We concluded that the sensitivity of the optical-fiber-based neutron detector can be roughly controlled by using the Li glass transparent composite scintillator.

As future work, we will consider the controllability of the size or sensitivity of this type of detector by fabricating optical-fiber-based neutron detectors with various scintillator sizes. In addition, the detailed detector energy response, such as the self-absorption effect, will be considered by a comparison between basic experiments and Monte Carlo simulations.

Acknowledgments

The experiment at UTR-KINKI of Kindai University was performed under a user research program.

References

1 W. H. Sweet: J. Neurooncol. **33** (1997) 19.
2 H. Tanaka, Y. Sakurai, T. Takata, T. Watanabe, S. Kawabata, M. Suzuki, S. I. Masunaga, K. Taki, K. Akabori, K. Watanabe, and K. Ono: Rev. Sci. Instrum **88** (2017) 056101. https://doi.org/10.1063/1.4982036
3 Y. Nakagawa, K. Pooh, T. Kobayashi, T. Kageji, S. Uyama, A. Matsumura and H. Kumada, J. Neurooncol. **62** (2033) 87.
4 H. Kumada, K. Saito, T. Sakae, A. Matsumura, T. Nakamura and K. Ono: Prog. Nucl. Sci. Technol. **2** (2011) 226.
5 T. Yanagida, A. Yamaji, N. Kawaguchi, Y. Fujimoto, K. Fukuda, S. Kurosawa, A. Yamazaki, K. Watanabe, Y. Futami, Y. Yokota, A. Yoshikawa, and M. Nikl: Appl. Phys. Express **4** (2011) 106401. https://doi.org/10.1143/APEX.4.106401
6 T. Yanagida, N. Kawaguchi, Y. Fujimoto, K. Fukuda, Y. Yokota, A. Yamazaki, K. Watanabe, J. Pejchal, A. Uritani, T. Iguchi, and A. Yoshikawa: Opt. Mater. (Amst) **33** (2011) 1243.
7 K. Watanabe, Y. Kawabata, A. Yamazaki, A. Uritani, T. Iguchi, K. Fukuda, and T. Yanagida: Nucl. Instruments Methods Phys. Res. Sect. A **802** (2015) 1.
8 D. Sugimoto, K. Watanabe, K. Hirota, A. Yamazaki, A. Uritani, T. Iguchi, K. Fukuda, S. Ishidu, N. Kawaguchi, T. Yanagida, Y. Fujimoto, A. Yoshikawa, H. Hasemi, K. Kino, and Y. Kiyanagi: Phys. Procedia **60** (2014) 349.
9 K. Watanabe, Y. Kondo, A. Yamazaki, A. Uritani, T. Iguchi, N. Kawaguchi, K. Fukuda, S. Ishizu, T. Yanagida, Y. Fujimoto, and A. Yoshikawa: Radiat. Meas. **71** (2014) 158.
10 K. Watanabe, T. Yamazaki, D. Sugimoto, A. Yamazaki, A. Uritani, T. Iguchi, K. Fukuda, S. Ishidu, T. Yanagida, and Y. Fujimoto: Nucl. Instruments Methods Phys. Res. Sect. A **784** (2015) 260.
11 A. Yamaji, T. Yanagida, N. Kawaguchi, Y. Yokota, Y. Fujimoto, S. Kurosawa, J. Pejchal, K. Watanabe, A. Yamazaki, and A. Yoshikawa: Radiat. Meas. **55** (2013) 132.
12 T. Yanagida, M. Koshimizu, Y. Fujimoto, K. Fukuda, K. Watanabe, G. Okada, and N. Kawaguchi: J. Lumin. **191** (2017) 22.
13 A. Ishikawa, A. Yamazaki, K. Watanabe, and S. Yoshihashi: Nucl. Inst. Methods Phys. Res. A **954** (2020) 161661.
14 A. Ishikawa, A. Yamazaki, K. Watanabe, S. Yoshihashi, A. Uritani, Y. Sakurai, H. Tanaka, R. Ogawara, M. Suda, and T. Hamano: Sens. Mater. **32** (2020) 1489.
15 A. Ishikawa, K. Watanabe, A. Yamazaki, and S. Yoshihashi: Nucl. Inst. Methods Phys. Res. A **1025** (2022) 166074.
16 A. Ishikawa, A. Yamazaki, K. Watanabe, S. Yoshihashi, A. Uritani, Y. Tsurita, K. Tsuchida, and Y. Kiyanagi: Radiat. Meas. **133** (2020) 106270. https://doi.org/10.1016/j.radmeas.2020.106270